Electrolytic reduction of $[Ru_2(C_3H_7COO)_4]Cl$ in solution did not give rise to extra peaks in the frozen-solution esr spectrum at 77 K. The black powdered material prepared in a similar way as the corresponding diruthenium tetraacetate[11] was close to being diamagnetic. This provides an indication that the ground state may be a singlet.

**Acknowledgment.** We thank the National Science Foundation for support under Grant No. 33142X. Professor A. W. Nolle, Department of Physics, University of Texas at Austin, very kindly permitted us to use his liquid helium facilities and Professor J. H. Lunsford assisted us in using the esr facilities in this department. Magnetic susceptibilities of solids were measured by Mrs. S. Kallesoe of Chemistry Laboratory I, the H. C. Orsted Institute, University of Copenhagen, Copenhagen, Denmark. E. P. acknowledges a leave of absence from the above institute, 1973–1974.

**Registry No.** $[Ru_2(C_3H_7COO)_4]Cl$, 53370-31-3.

## References and Notes

(1) T. A. Stephenson and G. Wilkinson, *J. Inorg. Nucl. Chem.*, **28**, 2285 (1966).
(2) M. J. Bennett, K. G. Caulton and F. A. Cotton, *Inorg. Chem.*, **8**, 1 (1969).
(3) F. A. Cotton and E. Pedersen, *Inorg. Chem.*, **14**, 383 (1975).
(4) E. Pedersen, *Acta Chem. Scand.*, **26**, 333 (1972).
(5) B. N. Figgis and R. S. Nyholm, *J. Chem. Soc.*, 4190 (1958).
(6) D. F. Evans, *J. Chem. Soc.*, 2003 (1959).
(7) B. N. Figgis and J. Lewis, *Progr. Inorg. Chem.*, **6**, 37 (1964).
(8) M. Suzuki, B. Tsujiyama, and S. Katsura, *J. Mol. Phys.*, **8**, 124 (1967).
(9) E. Pedersen and H. Toftlund, *Inorg. Chem.*, **13**, 1603 (1974).
(10) R. S. Nicholson, *Anal. Chem.*, **37**, 1351 (1965).
(11) P. Legzdins, R. W. Mitchell, G. L. Rempel, J. D. Ruddick, and G. Wilkinson, *J. Chem. Soc. A*, 3322 (1970).

---

Contribution from the Department of Chemistry, Texas A&M University, College Station, Texas 77843

# Magnetic and Electrochemical Properties of Transition Metal Complexes with Multiple Metal-to-Metal Bonds. III. Characterization of Tetrapotassium and Tripotassium Tetrasulfatodimolybdates

F. ALBERT COTTON,* BERTRAM A. FRENZ, ERIK PEDERSEN, and THOMAS R. WEBB

*Received June 25, 1974* AIC40408J

The compounds $K_4Mo_2(SO_4)_4 \cdot 2H_2O$ (**1**) and $K_3Mo_2(SO_4)_4 \cdot 3.5H_2O$ (**2**) have been prepared by reaction of $K_4Mo_2Cl_8$ with 0.1 *M* sulfuric acid at 25°. Both compounds have been identified and structurally characterized by X-ray crystallography. The former is the hydrate of a compound previously reported by Bowen and Taube; the latter is a new, paramagnetic compound. Compound **1** crystallizes in space group $C2/c$ with unit cell dimensions $a$ = 17.206 (3) Å, $b$ = 10.193 (2) Å, $c$ = 10.061 (2) Å, and $\beta$ = 94.92 (2)°, $Z$ = 4; 1217 reflections for which $F_o^2 > 3\sigma(F_o^2)$ were used to solve and refine the structure to $R_1$ = 0.028 and $R_2$ = 0.036. Compound **2** also crystallizes in space group $C2/c$. The unit cell dimensions are $a$ = 30.654 (4) Å, $b$ = 9.528 (1) Å, $c$ = 12.727 (1) Å, and $\beta$ = 97.43 (1)°, $Z$ = 8; 2341 reflections with $F_o^2 > 3\sigma(F_o^2)$ were used to solve and refine the structure to $R_1$ = 0.026 and $R_2$ = 0.033. The important structural unit in each compound is the $Mo_2(SO_4)_4^{n-}$ ion in which four bidentate sulfate ions, related by a fourfold axis, serve as bridges across the strongly bonded pair of molybdenum atoms. The $Mo_2(SO_4)_4^{4-}$ ion is diamagnetic with Mo–Mo = 2.111 (1) Å. The $Mo_2(SO_4)_4^{3-}$ ion is paramagnetic with one unpaired electron (1.65 ± 0.01 BM; $g_{av}$ = 1.90 ± 0.01) and an Mo–Mo distance of 2.164 (2) Å. From cyclic voltammetry and rotating-disk electrode polarography in 9 *M* $H_2SO_4$ it was shown that the two ions are related by a half-wave potential of +0.22 V *vs.* sce. The decomposition rate of $Mo_2(SO_4)_4^{3-}$ in solution is enormously variable, depending, *inter alia*, upon the condition of the electrode surfaces. By controlled-potential electrolysis a concentration sufficient for esr study was generated, and the following results were obtained: $g_{\parallel}$ = 1.891, $g_{\perp}$ = 1.909, $g_{av}$ = 1.903, $|A_{\parallel}| \times 10^4$ = 45.2 cm$^{-1}$, $|A_{\perp}| \times 10^4$ = 22.9 cm$^{-1}$, where the hyperfine coupling is to $^{95}$Mo.

## Introduction

There is now an enormous number of species containing the dimolybdenum(II) entity, with a quadruple Mo–Mo bond coordinated by ligands of very diverse types, for example $H_2O$, $Cl^-$, $CH_3^-$, $C_3H_5^-$, $PR_3$, $RCO_2^-$, etc.[1] A particularly important type of ligand is the bidentate bridging type which is sterically adapted to form two approximately parallel donor bonds, one to each of the two metal atoms in the Mo≡Mo group or other, similar, dinuclear coordination center. The carboxylato anions, $RCO_2^-$, are the commonest, but others include amidino ions, $R'NC(R)NR''^-$, triazino ions, $RNNNR'^-$, thiocarboxylato ions, $RCOS^-$, xanthato ions, $ROCS_2^-$, carbonate ion, $OCO_2^{2-}$, and sulfate ion, $O_2SO_2^{2-}$. The first $M_2(SO_4)_4^{n-}$ species reported was that postulated to occur in $K_4MO_2(SO_4)_4$ by Bowen and Taube.[2] In this laboratory the $Re_2(SO_4)_4^{2-}$ ion has been prepared and characterized as its sodium salt.[3]

We have previously reported[4] that X-ray crystallographic and Raman data for $K_4Mo_2(SO_4)_4 \cdot 2H_2O$, the hydrated form of Bowen and Taube's compound, verify the presence of the $Mo_2(SO_4)_4^{4-}$ ion and that the singly oxidized derivative, $Mo_2(SO_4)_4^{3-}$, can also be isolated and characterized crystallographically.[5] In this paper, we shall describe the structures of the two compounds $K_4Mo_2(SO_4)_4 \cdot 2H_2O$ and $K_3Mo_2(SO_4)_4 \cdot 3.5H_2O$ in full detail and also report on their redox properties and the bulk magnetic and electron spin resonance characteristics of the paramagnetic $Mo_2(SO_4)_4^{3-}$ ion.

## Experimental Section

**Preparation of Compounds.** The anhydrous compound $K_4Mo_2(SO_4)_4$ was prepared by the method of Bowen and Taube[2] with slight modifications. Crude $K_4Mo_2Cl_8$[6] (1.0 g) was stirred under nitrogen with 0.1 *M* $H_2SO_4$ (100 ml) at room temperature for 3 hr. The product was precipitated by adding excess solid $K_2SO_4$. The pink solid was filtered under nitrogen, washed with ethanol and ether, and dried for a few minutes under vacuum at room temperature.

Crystals of $K_3Mo_2(SO_4)_4 \cdot 3.5H_2O$ were obtained by slow diffusion of a saturated solution of $K_2SO_4$ in 0.1 *M* $H_2SO_4$ into a solution of $K_4Mo_2(SO_4)_4$ in 0.1 *M* $H_2SO_4$ through a medium-porosity sintered-glass disk under nitrogen in the apparatus described previously.[7] Crystals of the oxidized complex formed as bladelike, lavender needles, easily distinguishable from $K_4Mo_2(SO_4)_4$, which usually reprecipitated as a pink powder. The crystals appeared to be stable to air and moisture.

Satisfactory crystals of $K_4Mo_2(SO_4)_4 \cdot 2H_2O$ were also obtained by the diffusion method. However, it proved quite difficult to obtain a suitably crystalline product; very dilute solutions of $K_4Mo_2(SO_4)_4$ appeared to produce the best crystals. The crystals formed as rose red platelets which appeared to be air and moisture stable.

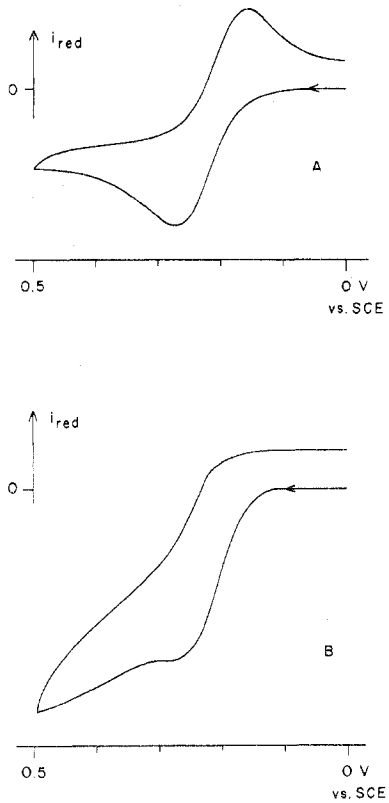


**Figure 1.** Cyclic voltammograms of approximately $10^{-3}$ *M* $Mo_2(SO_4)_4^{4-}$ in 9 *M* sulfuric acid, using a platinum-disk electrode: A, 100 mV $sec^{-1}$ (typical result independent of behavior at lower sweep rates); B, 5 mV $sec^{-1}$ (one of the many irreproducible voltammograms at low sweep rates).

**Electrochemical Measurements.** The instrumentation and general methods have been described earlier.[8] The only useful solvent for $K_4Mo_2(SO_4)_4 \cdot 2H_2O$ which we have found is aqueous sulfuric acid. The solubility in water is greatly increased by addition of hydrogen ions. Protonation of the sulfate ligands is therefore likely to be important. No solvents were found in which $K_3[Mo_2(SO_4)_4] \cdot 3.5H_2O$ could be dissolved faster than its own decomposition. Electrochemical reactions of $Mo_2(SO_4)_4^{4-}$ were studied at 25 ± 1° in the following solvents: (A) 0.2 *M* sulfuric acid saturated with sodium sulfate, (B) 6 *M* sulfuric acid, and (C) 9 *M* sulfuric acid. The potential ranges available were approximately 0 to 1 V *vs.* sce for a platinum electrode and −0.3 to +1 V *vs.* sce for carbon and gold electrodes.

Cyclic voltammetry on approximately $10^{-3}$ *M* carefully deoxygenated solutions of $K_4[Mo_2(SO_4)_4] \cdot 2H_2O$ showed the presence of an oxidation reaction. In solvent A the reaction observed at approximately +0.22 V *vs.* sce was completely irreversible, probably due to rapid decomposition of the oxidized product. This was independent of sweep rate and electrode material. The maximum sweep rate available was 500 mV $sec^{-1}$. In solvents B and C the results were almost identical. With platinum, gold, and carbon electrodes, sweep rates above 50 mV $sec^{-1}$, and switching potentials 200 mV above the oxidation current peak, a single-step quasireversible reaction was observed. The ratio between the cathodic and anodic peak currents, $i_p^c/i_p^a$, was unity and independent of the sweep rate $\nu$. The quantity $i_p^a\nu^{-1/2}$ was independent of $\nu$. The potential separation between the peaks, $\Delta E_p$, increased with $\nu$. $\Psi\nu^{1/2}$ was independent of $\nu$, where $\Psi$ is the reaction parameter for a quasireversible electron-transfer reaction, defined according to Nicholson.[9] At $\nu$ = 100 mV $sec^{-1}$, $\Delta E_p$ = 120 mV. The value of $E_{1/2}$ was +0.22 V *vs.* sce.

At sweep rates below 50 mV $sec^{-1}$ reproducible behavior could not be obtained because of variable rates of decomposition of the oxidized product. We were unable to find the reasons for this variation. Until we found that the results were very dependent upon the history of the electrode surfaces, which therefore require careful electrolytic cleaning in nitric acid, it was even impossible to obtain reproducible results from the same sample of $K_4[Mo_2(SO_4)_4] \cdot 2H_2O$. But even after this experimental improvement we found variable rates of decomposition into other electroactive species, thus giving rise to very complicated voltammograms. However, in two series of experiments with a platinum electrode in 9 *M* sulfuric acid with two different samples, we obtained identical and simple results with no indication of decomposition. These experiments gave the same value of $\Psi\nu^{1/2}$ as always obtained for fast sweeps. The ratio $i_p^a/i_p^c$ was independent of $\nu$ from 1 to 200 mV $sec^{-1}$, and $\Delta E_p$ was equal to 60 ± 2 mV for $\nu$ < 5 mV $sec^{-1}$; $E_{1/2}$ was equal to +0.22 V *vs.* sce. Because of the high viscosity of the solvent no diffusion effects were observed at the lowest sweep rates. Typical cyclic voltammograms are shown in Figure 1.

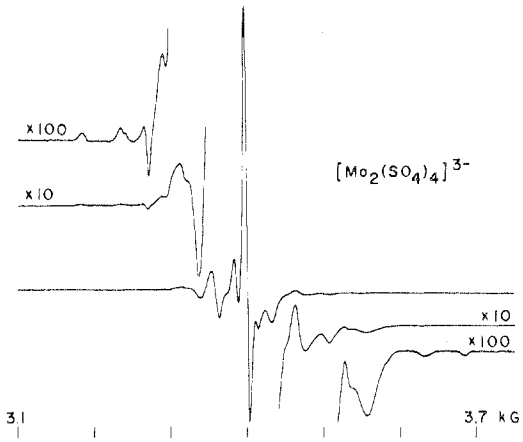


**Figure 2.** Esr spectrum of a frozen solution of $Mo_2(SO_4)_4^{3-}$ in 9 *M* sulfuric acid, at 9.085 GHz and 77 K.

Rotating-disk electrode polarography on the two well-behaved systems gave rise to plots of *E vs.* log $(i_L - i)/i$ having slopes with a limiting value of 60 ± 2 mV, reached for rotation rates below 5 $sec^{-1}$ with $\nu$ = 2 mV $sec^{-1}$.

The rate constant, *k*, for decomposition of $[Mo_2(SO_4)_4]^{3-}$ was estimated from cyclic voltammograms having $i_p^c/i_p^a \approx 0.5$ according to Nicholson and Shain.[10] The values of *k* thus found varied from >0.1 to $\ll 10^{-3}$ $sec^{-1}$.

Controlled-potential electrolytic oxidation of $Mo_2(SO_4)_4^{4-}$ was performed on one of the solutions having $k \ll 10^{-3}$ $sec^{-1}$. A rotating platinum-disk electrode at +0.30 V *vs.* sce was used. After decreases in current to 75 and 50% of the initial value small samples were removed for recording of frozen-solution esr spectra. The signal from the last sample was approximately twice as intense as from the first sample. The last sample was blue with a faint tinge of violet as expected from the color of solid $K_3[Mo_2(SO_4)_4] \cdot 3.5H_2O$. The visible absorption spectrum (400–700 nm) showed a broad maximum at 562 nm. The weak absorption due to residual $[Mo_2(SO_4)_4]^{4-}$ at 516 nm is not expected to be observable under these conditions. Similar experiments with solutions having larger values of *k* gave quite different results. A weak esr signal was observed, but the intensity did not increase with the amount of charge transferred, and the final products were either reddish violet or colorless solutions.

**Magnetic Susceptibilities.** Instrumentation and methods have been described previously.[8] Samples of $K_4[Mo_2(SO_4)_4] \cdot 2H_2O$ all showed weak, but varying, paramagnetism following the Curie law in the temperature range 60–300 K, corresponding to $\mu_{eff}$ values around 0.5 BM without corrections for diamagnetism. The intensities of the esr spectra of these powdered samples varied accordingly. The spectra were very similar to those obtained from the frozen solutions of electrolytically generated $[Mo_2(SO_4)]_4^{3-}$ discussed later. We therefore assume this to be a persistent impurity.

Pure samples of the blue $K_3[Mo_2(SO_4)_4] \cdot 3.5H_2O$ were prepared by removal of small amounts of the red $K_4[Mo_2(SO_4)_4] \cdot 2H_2O$ by repeated flotations in mixtures of bromoform and methanol, followed by manual removal of mixed-crystal conglomerates. Faraday measurements on two samples in the temperature range 60–300 K at fields of 2000, 5000, and 10,000 G showed the Curie law was strictly followed corresponding to $\mu$ = 1.65 ± 0.01 BM, including a diamagnetic correction of $-298 \times 10^{-6}$ cgsu per formula unit. This moment corresponds to $g_{av}$ = 1.90 ± 0.01, assuming the ground state to be a spin doublet.

**Electron Spin Resonance Spectra.** Instrumentation and methods were as previously described. The X- and Q-band spectra of frozen solutions of electrolytically generated $Mo_2(SO_4)_4^{3-}$ are shown in

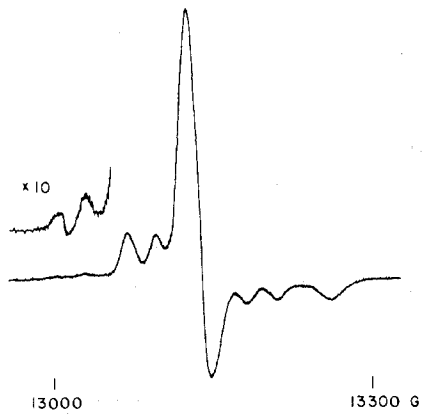


**Figure 3.** Esr spectrum of a frozen solution of $Mo_2(SO_4)_4^{3-}$ in 9 *M* sulfuric acid, at 35.10 GHz and ~85 K. The sensitivity of the spectrometer prevented detection of parallel orientation lines from complexes with $J = I^1 + I^2 > 0$.

Figures 2 and 3, respectively. The X-band spectrum of solid $K_3Mo_2(SO_4)_4 \cdot 3.5H_2O$ consists of a single broad and slightly anisotropic signal, 20 G wide and centered at $g = 1.91$. The X-band spectra of the solid and of frozen solutions of freshly prepared $K_4[Mo_2(SO_4)_4] \cdot 2H_2O$ were very similar or identical, respectively, to Figure 2, but with much lower intensities. This is attributed to slight contamination by $Mo_2(SO_4)_4^{3-}$, magnetically diluted in the crystals.

**X-Ray Crystallography. Data Collection for $K_3Mo_2(SO_4)_4 \cdot 3.5H_2O$.** A crystal of approximate dimensions 0.40 × 0.10 × 0.04 mm was mounted on a glass fiber with the long dimension parallel to $\phi$. Examination on a Syntex $P\bar{1}$ autodiffractometer[11] indicated that the crystal belonged to the monoclinic system; the systematic absences in the subsequent data set (*hkl* for $h + k$ odd, *h0l* for *l* odd) indicated possible space groups $C2/c$ or $Cc$. Accurate cell constants were obtained from least-squares refinement of the setting angles of 15 computer-centered reflections, giving $a = 30.654$ (4) Å, $b = 9.528$ (1) Å, $c = 12.727$ (1) Å, $\beta = 97.43$ (1)°, and $V = 3686$ (1) Å$^3$. For $Z = 8$, the calculated density is 2.73 g cm$^{-3}$, in good agreement with the value (2.72 ± 0.02 g cm$^{-3}$) determined by flotation in a mixture of bromoform and 1,4-diiodobutane.

Data were collected on the autodiffractometer[11] operated at 23 ± 1° using graphite-monochromatized Mo K$\alpha$ radiation. The $\theta$–$2\theta$ scan technique was employed, using a variable scan rate from 2 to 24° min$^{-1}$, depending on the intensity of the reflection, to collect 3583 unique reflections, of which 2341 were judged to be observed ($F_o^2 > 3\sigma(F_o^2)$), in the range $0° < 2\theta < 48°$. The scan range was from 0.7° below the K$\alpha_1$ peak to 0.7° above the K$\alpha_2$ peak. The intensities of four standard reflections, re-collected every 96 reflections, underwent no significant change during data collection.

No effects owing to secondary extinction were observed in the data set. The linear absorption coefficient is 25.3 cm$^{-1}$ for Mo K$\alpha$ radiation. The transmission factors for the minimum and maximum path lengths were calculated to be 0.98 and 0.78. No absorption correction was made because the crystal was accidentally dislodged from the fiber before it could be accurately measured. The parameter $p$ used in calculating $\sigma(F_o^2)$ was set at 0.04.

**Data Collection for $K_4Mo_2(SO_4)_4 \cdot 2H_2O$.** A platelet of dimensions 0.15 × 0.14 × 0.03 mm was mounted on a glass fiber. Preliminary precession photographs indicated that the crystals belonged to a nonprimitive space group in the monoclinic system. Systematic absences in the subsequent data set (*hkl* for $h + k$ odd, *h0l* for *l* odd) indicated as possible space groups $C2/c$ and $Cc$. Cell constants were obtained by a least-squares refinement of 15 carefully centered reflections in the range $25° < 2\theta < 35°$, giving $a = 17.206$ (3) Å, $b = 10.193$ (2) Å, $c = 10.061$ (2) Å, $\beta = 94.92$ (2)°, and $V = 1758$ (1) Å$^3$. The small amount of crystalline material precluded a direct density determination; however, a comparison of the cell volume with that of $K_3Mo_2(SO_4)_4 \cdot 3.5H_2O$ suggested $Z = 4$, a formulation that would impose $C_i$ ($\bar{1}$) or $C_2$ (2) symmetry on the anion if $C2/c$ were the space group. The calculated density is 2.90 g cm$^{-3}$.

Data were collected at 19 ± 1° on a Syntex $P\bar{1}$ autodiffractometer using Mo K$\alpha$ radiation as described previously.[11] Data were collected in the range $0° < 2\theta < 50°$, using the $\theta$–$2\theta$ scan technique with a variable scan rate (2.0–24.0° min$^{-1}$) and a scan range from $2\theta$ (K$\alpha_1$) − 0.7° to $2\theta$ (K$\alpha_2$) + 0.7°. A total of 1549 reflections were collected, of which 1217 had $F_o^2 > 3\sigma(F_o^2)$. The parameter $p$ used in calculating[11] $\sigma(F_o^2)$ was set equal to 0.04. Four standard reflections, remeasured every 96 reflections, did not change significantly in intensity. The linear absorption coefficient is 28.7 cm$^{-1}$; because of the platelike form of the data crystal, a numerical absorption correction was applied to the data. Calculated transmission factors ranged from 0.643 to 0.910, with the average value 0.835. No extinction correction was necessary.

**Solution and Refinement[12] of $K_3Mo_2(SO_4)_4 \cdot 3.5H_2O$ Structure.** Although the assumption that $Z = 8$ does not require that the complex ion possess crystallographic symmetry, the sharpened Patterson function was most readily interpreted in terms of two nonequivalent dinuclear units, one centered on the 4c position (1/4, 1/4, 0) and one on the 4a position (0, 0, 1/2) of space group $C2/c$. The positions of the two independent Mo atoms were varied in two cycles of full-matrix least-squares refinement to $R_1 = \sum \| F_o| - |F_c| \| / \sum |F_o| = 0.44$ and $R_2 = \sum w(|F_o| - |F_c|)^2 / \sum w F_o^2 = 0.54$. The structure was elaborated by several difference Fourier syntheses followed by refinement of positional and thermal parameters. Anisotropic refinement converged to values of $R_1$ and $R_2$ of 0.028 and 0.036, respectively.

A difference Fourier map contained several peaks of electron density 1.5 e Å$^{-3}$ or less. Many of these peaks were located near Mo, K, or S atoms; however, seven such peaks could be identified as the hydrogen atoms of water molecules on the basis of their positions relative to other atoms in the structure. The hydrogen atom positions were varied with isotropic thermal parameters fixed at 4.0 Å$^2$.

Least-squares refinement of the 279 variables converged at $R_1 = 0.026$ and $R_2 = 0.033$. The error in an observation of unit weight is 1.12. The function minimized was $\sum w(|F_o| - |F_c|)^2$, where the weight, $w$, is $4F_o^2/\sigma^2(F_o^2)$. Scattering factors of Cromer and Waber[13] were used, with hydrogen scattering factors from Stewart, Davidson, and Simpson.[14] Anomalous dispersions for Mo, K, and S were included in calculations of $F_c$,[15] with values taken from Cromer and Liberman.[16] No unusual trends were observed in an analysis of $\sum w(|F_o| - |F_c|)^2$ as a function of reflection number, $\lambda^{-1} \sin \theta$, $|F_o|$, or various classes of indices.

The observed and calculated structure factor amplitudes are listed in Table I.[17] The atomic positional parameters are given in Table II; anisotropic thermal parameters for nonhydrogen atoms are given in Table III. Table IV lists root-mean-square amplitudes of thermal vibration.

**Solution and Refinement[12] of $K_4Mo_2(SO_4)_4 \cdot 2H_2O$ Structure.** The three-dimensional Patterson function suggested locating the $Mo_2$ entity on the 4c position (1/4, 1/4, 0) in space group $C2/c$. Two cycles of refinement on the independent Mo atom produced $R_1 = 0.46$ and $R_2 = 0.54$. The structure was elaborated by difference Fourier syntheses and refinement of positional and thermal parameters. An examination of $w(|F_o| - |F_c|)^2$ *vs.* $|F_o|$ indicated that $p$ had been set too low; it was changed to 0.05 for the last cycles of refinement. The conventional and weighted residuals were 0.034 and 0.043, respectively.

A difference Fourier map at this stage contained a number of peaks of electron density 1 e Å$^{-3}$, mostly around the Mo atom. However, it was again possible to identify the hydrogen atoms. After refining their positions, two cycles of full-matrix refinement of all atoms (isotropic on H, anisotropic on all others) were carried out, at which point the structure had converged with $R_1 = 0.028$ and $R_2 = 0.036$. The error in an observation of unit weight was 0.98. No systematic trends in the data were observed as a function of reflection number, $\lambda^{-1} \sin \theta$, $|F_o|$, or indices.

The observed and calculated structure factors are listed in Table V.[17] The atomic positional parameters appear in Table VI and thermal parameters appear in Table VII. Table VIII gives root-mean-square amplitudes of thermal vibration.

## Structural Results

**$K_4Mo_2(SO_4)_4 \cdot 2H_2O$.** The structure of the $Mo_2(SO_4)_4^{4-}$ ion is shown in Figure 4. It is seen to consist of the $Mo_2^{4+}$ unit coordinated equatorially by four bidentate sulfate ions and axially by terminal oxygen atoms from neighboring sulfate ions. This bridging pattern leads to the infinite, two-dimensional network shown in Figure 5, a stereoscopic view of the unit cell. The crystallographic symmetry of the ion is $C_i$ ($\bar{1}$); however, the virtual symmetry is $C_{4h}$ (4/*m*), reduced from $D_{4h}$ (4/*mmm*) by the folds in the Mo–Mo–O–S–O rings.

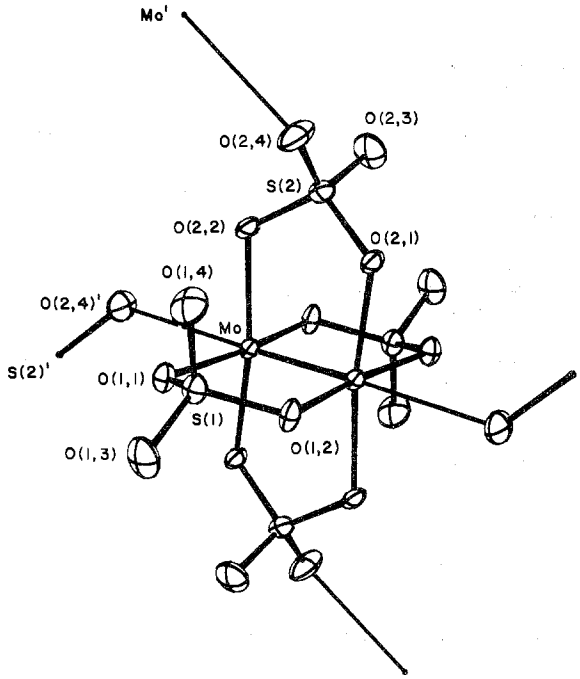


**Figure 4.** Structure of the $Mo_2(SO_4)_4^{4-}$ ion, showing the polymerization of the complex. The atom-numbering scheme used for both structures is defined. Ellipsoids enclose 50% of the electron density.

The potassium ions occur in three sets. One eightfold set occupies a general position, but the others occur in two sets lying on twofold axes at the 4e position (0, $y$, $^1/_4$) ($y$ = +0.34 and −0.07, respectively, for the two sets). Sulfate and water oxygen atoms make up the coordination polyhedron around the potassium ions. The water molecules are hydrogen bonded to sulfate oxygen atoms.

The structure presents a layered appearance, with sheets of potassium and oxygen atoms alternating with molybdenum-containing layers stacked in the $a$ direction, which corresponds to the thin dimension of the platelet.

Bond distances and angles are listed in Tables IX and X. The distances and angles around Mo appear normal in comparison with related structures.[18-20] The sulfate ion has undergone some distortion; the magnitude of this distortion is similar to or slightly greater than that found for other examples of bridging bidentate sulfate.[21]

**$K_3Mo_2(SO_4)_4 \cdot 3.5H_2O$.** The structure of the complex ion $Mo_2(SO_4)_4^{3-}$ is pictured in Figure 6. Its structure is very similar to that of the $Mo_2(SO_4)_4^{4-}$ ion except for the presence of coaxial water molecules here, as opposed to sulfate oxygen atoms in the 4− ion. Although there are two crystallographically distinct $Mo_2(SO_4)_4^{3-}$ ions in the structure, the bond distances and angles (Tables XI and XII) differ very little in the two complexes. The nonequivalence results from differences in the packing. Complex **1** (4c) packs as isolated units, whereas complex **2** (4a) forms an infinite chain parallel to the $c$ axis. The terminal water molecule in complex **2** lies on a crystallographic twofold axis (0, 0.18, $^1/_4$) and bridges dimers centered at (0, 0, 0) and (0, 0, $^1/_2$). The packing is shown in Figure 7, a stereoscopic view of the contents of the unit cell.

**Table II.** Atomic Positional Parameters for $K_3Mo_2(SO_4)_4 \cdot 3.5H_2O$[a]

| Atom | $x$ | $y$ | $z$ |
|---|---|---|---|
| | Molecule 1 | | |
| Mo | 0.22389 (1) | 0.24931 (4) | 0.04984 (3) |
| S(1) | 0.19270 (4) | 0.4134 (1) | −0.1607 (1) |
| S(2) | 0.21434 (4) | −0.0082 (1) | −0.1041 (1) |
| O(1,1) | 0.2367 (1) | 0.3476 (4) | −0.1747 (3) |
| O(1,2) | 0.1787 (1) | 0.3461 (4) | −0.0619 (3) |
| O(1,3) | 0.1613 (1) | 0.3799 (4) | −0.2513 (3) |
| O(1,4) | 0.1991 (1) | 0.5623 (4) | −0.1423 (3) |
| O(2,1) | 0.2578 (1) | 0.0602 (4) | −0.1202 (3) |
| O(2,2) | 0.2015 (1) | 0.0564 (4) | −0.0031 (3) |
| O(2,3) | 0.1816 (1) | 0.0258 (4) | −0.1932 (3) |
| O(2,4) | 0.2205 (1) | 0.1560 (4) | −0.0859 (3) |
| O(T1)[b] | 0.1711 (1) | 0.2568 (5) | 0.1890 (3) |
| H(1) | 0.172 (3) | 0.176 (10) | 0.222 (7) |
| H(2) | 0.182 (3) | 0.299 (10) | 0.230 (7) |
| | Molecule 2 | | |
| Mo | 0.00281 (1) | 0.04341 (5) | 0.42270 (3) |
| S(1) | 0.09850 (4) | −0.0052 (1) | 0.5464 (1) |
| S(2) | −0.00355 (4) | 0.2861 (1) | 0.5878 (1) |
| O(1,1) | 0.0699 (1) | 0.0677 (4) | 0.4515 (3) |
| O(1,2) | 0.0638 (1) | −0.0249 (4) | 0.6272 (3) |
| O(1,3) | 0.1103 (1) | −0.1396 (4) | 0.5137 (3) |
| O(1,4) | 0.1300 (1) | 0.0892 (4) | 0.5914 (3) |
| O(2,1) | −0.0057 (1) | 0.2483 (4) | 0.4717 (3) |
| O(2,2) | −0.0129 (1) | 0.1488 (4) | 0.6426 (3) |
| O(2,3) | −0.0390 (1) | 0.3827 (4) | 0.6001 (3) |
| O(2,4) | 0.0395 (1) | 0.3357 (4) | 0.6289 (3) |
| O(T2)[b] | 0 | 0.1798 (6) | $^1/_4$ |
| H(3) | 0.019 (3) | 0.216 (9) | 0.250 (8) |
| | Other Atoms | | |
| K(1) | 0.21463 (4) | 0.1757 (1) | −0.3601 (1) |
| K(2) | 0.09849 (4) | 0.1810 (1) | −0.2097 (1) |
| K(3) | 0.09767 (5) | 0.4264 (2) | 0.0889 (1) |
| O(1) | 0.0647 (2) | 0.3791 (5) | 0.2816 (4) |
| O(2) | 0.1265 (2) | 0.3525 (5) | 0.4667 (4) |
| H(4) | 0.151 (3) | 0.361 (10) | 0.450 (7) |
| H(5) | 0.126 (3) | 0.279 (10) | 0.491 (8) |
| H(6) | 0.087 (3) | 0.353 (9) | 0.339 (7) |
| H(7) | 0.051 (3) | 0.419 (11) | 0.293 (8) |

[a] Numbers in parentheses are estimated standard deviations in the last significant figure in this and all other tables. [b] (T) refers to the terminal water molecules.

## Discussion

The two anions $Mo_2(SO_4)_4^{4-}$ and $Mo_2(SO_4)_4^{3-}$ constitute the first pair of dinuclear, multiply bonded, isostructural complexes with electronic configurations differing by one

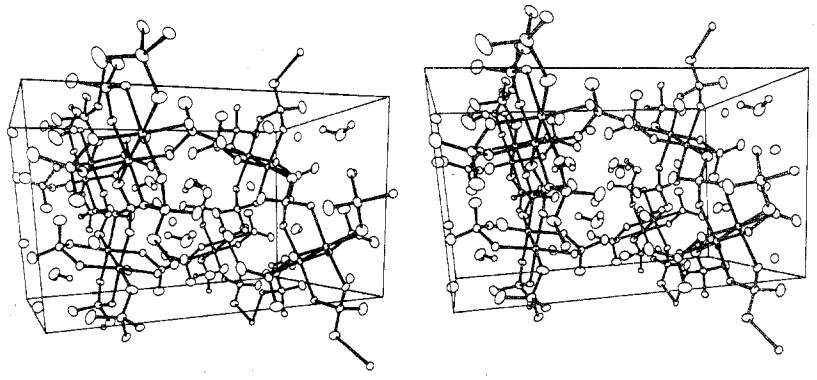

**Figure 5.** Stereoscopic view of the unit cell contents of $K_4Mo_2(SO_4)_4 \cdot 2H_2O$. The temperature factors for H atoms have been set at 1.0 Å$^2$.

**Table III.** Anisotropic Thermal Parameters for $K_3Mo_2(SO_4)_4 \cdot 3.5H_2O$[a,b]

| Atom | $\beta_{11}$ | $\beta_{22}$ | $\beta_{33}$ | $\beta_{12}$ | $\beta_{13}$ | $\beta_{23}$ |
|---|---|---|---|---|---|---|
| | | | Molecule 1 | | | |
| Mo | 36.5 (5) | 240 (5) | 171 (3) | 6 (1) | 21.1 (8) | −2 (3) |
| S(1) | 45 (1) | 312 (13) | 213 (8) | 3 (3) | 5 (3) | 13 (8) |
| S(2) | 49 (1) | 277 (13) | 233 (8) | −3 (3) | 9 (3) | −23 (8) |
| O(1,1) | 50 (4) | 482 (43) | 196 (22) | 15 (11) | 23 (7) | 57 (25) |
| O(1,2) | 41 (4) | 418 (41) | 268 (24) | 20 (10) | 17 (8) | 90 (25) |
| O(1,3) | 58 (4) | 641 (47) | 303 (25) | −21 (12) | −19 (8) | 21 (28) |
| O(1,4) | 71 (5) | 303 (40) | 345 (26) | −18 (11) | 27 (9) | −2 (27) |
| O(2,1) | 68 (5) | 391 (42) | 279 (24) | −21 (11) | 42 (8) | −119 (26) |
| O(2,2) | 45 (4) | 360 (39) | 282 (23) | −10 (10) | 37 (8) | −46 (25) |
| O(2,3) | 66 (5) | 709 (50) | 275 (25) | 22 (12) | −14 (8) | 41 (29) |
| O(2,4) | 85 (5) | 198 (39) | 380 (26) | 14 (11) | 43 (9) | 2 (25) |
| O(T1) | 71 (5) | 721 (55) | 274 (27) | −3 (14) | 28 (9) | −68 (30) |
| | | | Molecule 2 | | | |
| Mo | 35.3 (5) | 380 (6) | 144 (3) | 0.3 (12) | 6.7 (9) | 19 (3) |
| S(1) | 33 (1) | 578 (16) | 243 (8) | −5 (4) | 3 (3) | −23 (9) |
| S(2) | 61 (2) | 418 (15) | 246 (9) | 4 (4) | 6 (3) | −49 (9) |
| O(1,1) | 38 (4) | 603 (45) | 324 (25) | −11 (11) | 21 (8) | 90 (27) |
| O(1,2) | 39 (4) | 679 (47) | 199 (22) | 4 (11) | 4 (7) | 38 (27) |
| O(1,3) | 63 (5) | 674 (50) | 419 (28) | 48 (12) | 28 (9) | 4 (30) |
| O(1,4) | 46 (4) | 799 (51) | 358 (26) | −50 (12) | 2 (8) | −107 (30) |
| O(2,1) | 83 (5) | 399 (41) | 198 (23) | 15 (12) | 6 (8) | 1 (27) |
| O(2,2) | 67 (4) | 574 (45) | 131 (22) | −18 (11) | 38 (8) | 8 (25) |
| O(2,3) | 94 (5) | 627 (50) | 417 (28) | 84 (13) | 24 (10) | −48 (31) |
| O(2,4) | 77 (5) | 861 (54) | 387 (28) | −86 (13) | −29 (10) | −3 (32) |
| O(T2) | 68 (7) | 481 (69) | 220 (34) | 0 | 13 (14) | 0 |
| | | | Other Atoms | | | |
| K(1) | 57 (1) | 676 (15) | 325 (8) | −48 (4) | 27 (3) | −133 (9) |
| K(2) | 66 (1) | 783 (16) | 347 (8) | −25 (4) | 36 (3) | −35 (10) |
| K(3) | 105 (2) | 891 (18) | 428 (9) | 41 (5) | 3 (3) | 46 (11) |
| O(1) | 100 (7) | 715 (61) | 606 (37) | 19 (15) | 24 (12) | −148 (38) |
| O(2) | 115 (7) | 871 (65) | 772 (44) | −56 (18) | 82 (14) | 156 (41) |

[a] The form of the anisotropic thermal ellipsoid is $\exp[-10^5(\beta_{11}h^2 + \beta_{22}k^2 + \beta_{33}l^2 + 2\beta_{12}hk + 2\beta_{13}hl + 2\beta_{23}kl)]$. [b] Hydrogen atoms were assigned a fixed isotropic temperature parameter of 4.0 Å$^2$.

**Table IV.** Rms Components of Thermal Displacement (Å) for $K_3Mo_2(SO_4)_4 \cdot 3.5H_2O$

| | | | |
|---|---|---|---|
| | | Molecule 1 | |
| Mo | 0.104 (1) | 0.112 (1) | 0.134 (1) |
| S(1) | 0.119 (3) | 0.131 (2) | 0.148 (2) |
| S(2) | 0.112 (3) | 0.138 (2) | 0.153 (2) |
| O(1,1) | 0.118 (8) | 0.144 (7) | 0.161 (6) |
| O(1,2) | 0.120 (8) | 0.138 (7) | 0.163 (6) |
| O(1,3) | 0.139 (7) | 0.167 (7) | 0.190 (6) |
| O(1,4) | 0.116 (8) | 0.165 (6) | 0.184 (6) |
| O(2,1) | 0.112 (8) | 0.154 (7) | 0.187 (6) |
| O(2,2) | 0.124 (8) | 0.134 (7) | 0.164 (6) |
| O(2,3) | 0.137 (7) | 0.180 (6) | 0.190 (6) |
| O(2,4) | 0.095 (9) | 0.169 (6) | 0.202 (6) |
| O(T1) | 0.142 (8) | 0.182 (7) | 0.187 (7) |
| | | Molecule 2 | |
| Mo | 0.107 (1) | 0.129 (1) | 0.133 (1) |
| S(1) | 0.123 (3) | 0.143 (2) | 0.164 (2) |
| S(2) | 0.129 (3) | 0.149 (2) | 0.172 (2) |
| O(1,1) | 0.128 (7) | 0.149 (7) | 0.181 (6) |
| O(1,2) | 0.123 (7) | 0.138 (7) | 0.178 (6) |
| O(1,3) | 0.151 (7) | 0.183 (6) | 0.194 (6) |
| O(1,4) | 0.130 (8) | 0.172 (6) | 0.204 (6) |
| O(2,1) | 0.126 (8) | 0.134 (7) | 0.199 (6) |
| O(2,2) | 0.094 (9) | 0.160 (6) | 0.181 (6) |
| O(2,3) | 0.145 (8) | 0.185 (6) | 0.227 (6) |
| O(2,3) | 0.144 (7) | 0.187 (6) | 0.232 (6) |
| O(T2) | 0.133 (10) | 0.149 (11) | 0.179 (9) |
| | | Other Atoms | |
| K(1) | 0.138 (2) | 0.156 (2) | 0.199 (2) |
| K(2) | 0.160 (2) | 0.173 (2) | 0.197 (2) |
| K(3) | 0.178 (2) | 0.202 (2) | 0.231 (2) |
| O(1) | 0.168 (8) | 0.215 (7) | 0.233 (7) |
| O(2) | 0.173 (8) | 0.238 (7) | 0.259 (7) |

**Table VI.** Positional Parameters for $K_4Mo_2(SO_4)_4 \cdot 2H_2O$

| | $x$ | $y$ | $z$ |
|---|---|---|---|
| Mo | 0.24845 (3) | 0.29129 (4) | 0.09597 (4) |
| K(1) | 0 | 0.3458 (1) | 1/4 |
| K(2) | 0.1448 (1) | 0.3612 (1) | −0.4096 (2) |
| K(3) | 0 | 0.0704 (2) | −1/4 |
| S(1) | 0.4150 (1) | 0.1654 (1) | 0.0671 (1) |
| S(2) | 0.2957 (1) | 0.5112 (1) | −0.1054 (1) |
| O(1,1) | 0.3704 (2) | 0.2595 (4) | 0.1483 (4) |
| O(1,2) | 0.3732 (2) | 0.1623 (4) | −0.0719 (4) |
| O(1,3) | 0.4934 (2) | 0.2149 (5) | 0.0593 (4) |
| O(1,4) | 0.4128 (3) | 0.0357 (4) | 0.1251 (5) |
| O(2,1) | 0.2697 (2) | 0.4858 (4) | 0.0314 (3) |
| O(2,2) | 0.2738 (2) | 0.3926 (4) | −0.1897 (3) |
| O(2,3) | 0.3791 (3) | 0.5288 (5) | −0.0968 (5) |
| O(2,4) | 0.2546 (3) | 0.6271 (4) | −0.1594 (4) |
| O(3) | 0.0916 (3) | 0.1575 (6) | 0.3505 (6) |
| H(1) | 0.093 (4) | 0.119 (9) | 0.421 (9) |
| H(2) | 0.135 (5) | 0.146 (8) | 0.321 (8) |

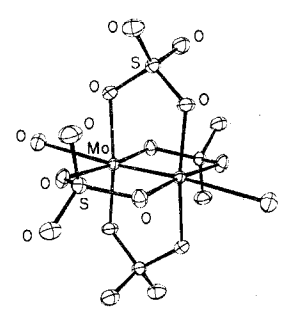


**Figure 6.** Structure of the $Mo_2(SO_4)_4^{3-}$ ion with terminal water molecules. Ellipsoids enclose 50% of the electron density.

electron which have been isolated. On the basis of previously published discussions of the quadruple bond[22-24] we would expect the difference in electron population to occur in the $\delta$ orbital, with $Mo_2(SO_4)_4^{4-}$ having the full quadruple bond $\sigma^2\pi^4\delta^2$ and $Mo_2(SO_4)_4^{3-}$ having a bond of order 3.5 with the configuration $\sigma^2\pi^4\delta$. The results reported here serve to

**Table VII.** Thermal Parameters for All Atoms in $K_4Mo_2(SO_4)_4 \cdot 2H_2O$[a]

| | $\beta_{11}$ or $B_{iso}$ | $\beta_{22}$ | $\beta_{33}$ | $\beta_{12}$ | $\beta_{13}$ | $\beta_{23}$ |
|---|---|---|---|---|---|---|
| Mo | 8.1 (2) | 27.5 (5) | 19.3 (5) | 0.9 (2) | 1.0 (2) | 1.0 (4) |
| K(1) | 18.2 (7) | 49 (2) | 59 (2) | 0 | −1.4 (9) | 0 |
| K(2) | 16.1 (5) | 66 (2) | 78 (2) | −6.2 (7) | −3.6 (7) | 25 (1) |
| K(3) | 19.8 (8) | 58 (2) | 94 (3) | 0 | 19 (1) | 0 |
| S(1) | 8.8 (5) | 44 (1) | 36 (1) | 3.7 (6) | −0.2 (6) | −2 (1) |
| S(2) | 15.1 (5) | 38 (1) | 30 (1) | −4.0 (6) | 5.6 (6) | 3 (1) |
| O(1,1) | 11 (1) | 47 (4) | 32 (4) | 3 (2) | −2 (2) | −5 (3) |
| O(1,2) | 10 (1) | 58 (4) | 21 (4) | 5 (2) | 0 (2) | −9 (3) |
| O(1,3) | 9 (1) | 89 (6) | 70 (5) | −1 (2) | 1 (2) | −17 (4) |
| O(1,4) | 27 (2) | 48 (5) | 66 (5) | 9 (2) | −7 (2) | 11 (4) |
| O(2,1) | 15 (1) | 33 (4) | 20 (4) | 0 (2) | 3 (2) | 1 (3) |
| O(2,2) | 17 (1) | 38 (4) | 20 (4) | −3 (2) | 6 (2) | 4 (3) |
| O(2,3) | 16 (2) | 103 (6) | 64 (5) | −18 (3) | 13 (2) | −16 (5) |
| O(2,4) | 38 (2) | 43 (4) | 39 (4) | 8 (2) | 3 (2) | 15 (4) |
| O(3) | 29 (2) | 130 (8) | 73 (7) | 29 (3) | 17 (3) | 36 (6) |
| H(1)[b] | 2 (2) | | | | | |
| H(2)[b] | 2 (2) | | | | | |

[a] The form of the anisotropic thermal ellispoid is $\exp[-10^{-4}(\beta_{11}h^2 + \beta_{22}k^2 + \beta_{33}l^2 + 2\beta_{12}hk + 2\beta_{13}hl + 2\beta_{23}kl)]$. [b] $B_{iso}$ (Å$^2$).

**Table VIII.** Rms Components of Thermal Displacement (Å) of $K_4Mo_2(SO_4)_4 \cdot 2H_2O$

| | | | |
|---|---|---|---|
| Mo | 0.099 (1) | 0.109 (1) | 0.121 (1) |
| K(1) | 0.158 (3) | 0.161 (3) | 0.182 (3) |
| K(2) | 0.147 (2) | 0.156 (2) | 0.231 (2) |
| K(3) | 0.146 (4) | 0.176 (3) | 0.232 (3) |
| S(1) | 0.110 (3) | 0.136 (3) | 0.156 (2) |
| S(2) | 0.113 (3) | 0.140 (3) | 0.159 (2) |
| O(1,1) | 0.116 (8) | 0.133 (8) | 0.162 (7) |
| O(1,2) | 0.098 (10) | 0.119 (8) | 0.180 (6) |
| O(1,3) | 0.118 (9) | 0.176 (7) | 0.227 (7) |
| O(1,4) | 0.131 (9) | 0.189 (7) | 0.220 (7) |
| O(2,1) | 0.100 (10) | 0.131 (8) | 0.150 (7) |
| O(2,2) | 0.090 (10) | 0.142 (8) | 0.164 (7) |
| O(2,3) | 0.120 (9) | 0.174 (8) | 0.254 (7) |
| O(2,4) | 0.115 (10) | 0.166 (8) | 0.240 (7) |
| O(3) | 0.162 (10) | 0.169 (10) | 0.302 (8) |

characterize the two complexes in several important ways: (1) structurally; (2) in terms of their electrochemical relationship, which includes as well some information on the kinetic stability of $Mo_2(SO_4)_4^{3-}$ in solution; (3) magnetically, including some of the principal parameters in the spin Hamiltonian. Each of these points will now be discussed, in the order mentioned.

**Structural Comparison.** The two structures are related in a manner which is in accord with their expected electronic configurations. Qualitatively, the structures of the two complex anions $Mo_2(SO_4)_4^{4-}$ and $Mo_2(SO_4)_4^{3-}$ are identical. Evidently the combined effect of (a) the presence of one $\delta$ electron and (b) the rigidifying effect of the sulfato bridges causes retention of the eclipsed rotational structure in the $Mo_2(SO_4)_4^{3-}$ ion. There are, however, two noteworthy quantitative changes.

First, the Mo–Mo distance increases from 2.111 (1) Å in the $Mo_2(SO_4)_4^{4-}$ ion to 2.164 (2) Å in the $Mo_2(SO_4)_4^{3-}$ ion, a change of 0.053 (3) Å. This may be attributed to loss of half of the $\delta$ bond. This is a reasonable number based on the original correlation[22] of bond distance with bond order for bonds between metal atoms of the second and third transition series, according to which a change of 1 unit in bond order, from 3 to 4, would cause a change of about 0.10 Å in bond distance.

Second, the Mo–$OSO_3$ bond lengths decrease from an average of 2.14 ± 0.0 Å in $Mo_2(SO_4)_4^{4-}$ to an average of 2.06 ± 0.01 Å in $Mo_2(SO_4)_4^{3-}$. The direction of the change accords with the fact that increasing the formal oxidation number of the metal atoms (by $^1/_2$) should decrease their radius.

Finally, it may be noted that in neither case is the binding of coaxial ligands very strong. In $K_4Mo_2(SO_4)_4 \cdot 2H_2O$ the coaxially bound oxygen atoms are from sulfato groups of neighboring anions, as shown in Figure 5, while in $K_3Mo_2(SO_4)_4 \cdot 3.5H_2O$ the coaxial positions are occupied by water molecules. These long Mo–O distances range from 2.55 to 2.60 Å.

**Electrochemical Properties.** The results of the electrochemical studies are interpreted in terms of the following reaction scheme of eq 1, where X and Y are unidentified

$$\begin{array}{ccc} [Mo_2(SO_4)_4]^{3-} + e^- & \xrightleftharpoons[vs.\ sce]{E_{1/2} = +0.22\ V} & [Mo_2(SO_4)_4]^{4-} \\ \downarrow k & & \downarrow \text{slow} \\ X & & Y \end{array} \quad (1)$$

decomposition products. The rate constant, $k$, for decomposition of $Mo_2(SO_4)_4^{3-}$ was estimated from cyclic voltammograms having $i_p^c/i_p^a \approx 0.5$, but the results vary widely, from $10^{-3}$ sec$^{-1}$ or less to 0.1 sec$^{-1}$ or more, depending apparently upon the catalytic effect of the electrode surfaces and possibly on other factors as well.

**Magnetic and Electron Spin Resonance Properties.** The $Mo_2(SO_4)_4^{4-}$ ion would be expected to be diamagnetic unless there is significant temperature-independent paramagnetism. All samples of $K_4Mo_2(SO_4)_4 \cdot 2H_2O$ showed weak paramagnetism, but this had a Curie law dependence on temperature. The samples also showed esr signals consistent with the presence of $Mo_2(SO_4)_4^{3-}$ ions, which varied in intensity in qualitative accord with the paramagnetism. We believe that the $Mo_2(SO_4)_4^{4-}$ ion is truly diamagnetic but that $K_4Mo_2(SO_4)_4 \cdot 2H_2O$ is normally contaminated by $Mo_2(SO_4)_4^{3-}$ ions which are responsible for the observed temperature-dependent paramagnetism.

As reported earlier, $K_3Mo_2(SO_4)_4 \cdot 3.5H_2O$ showed paramagnetism roughly in accord with one unpaired electron per formula unit.[5] This has now been confirmed and measure-

**Table IX.** Bond Distances (Å) in $K_4Mo_2(SO_4)_4 \cdot 2H_2O$[a]

| | | | | | |
|---|---|---|---|---|---|
| Mo–Mo | 2.111 (1) | S(1)–O(1,1) | 1.511 (4) | S(2)–O(2,2) | 1.506 (4) |
| Mo–O(1,1) | 2.143 (4) | S(1)–O(1,2) | 1.517 (4) | S(2)–O(2,3) | 1.441 (4) |
| Mo–O(1,2) | 2.139 (4) | S(1)–O(1,3) | 1.450 (4) | S(2)–O(2,4) | 1.458 (4) |
| Mo–O(2,1) | 2.127 (4) | S(1)–O(1,4) | 1.448 (4) | O(3)–H(1) | 0.81 (9) |
| Mo–O(2,2) | 2.148 (4) | S(2)–O(2,1) | 1.506 (4) | O(3)–H(2) | 0.83 (9) |
| Mo–O(2,4)′ | 2.591 (4) | | | | |

[a] Prime denotes an atom in another $Mo_2(SO_4)_4^{4-}$ unit.

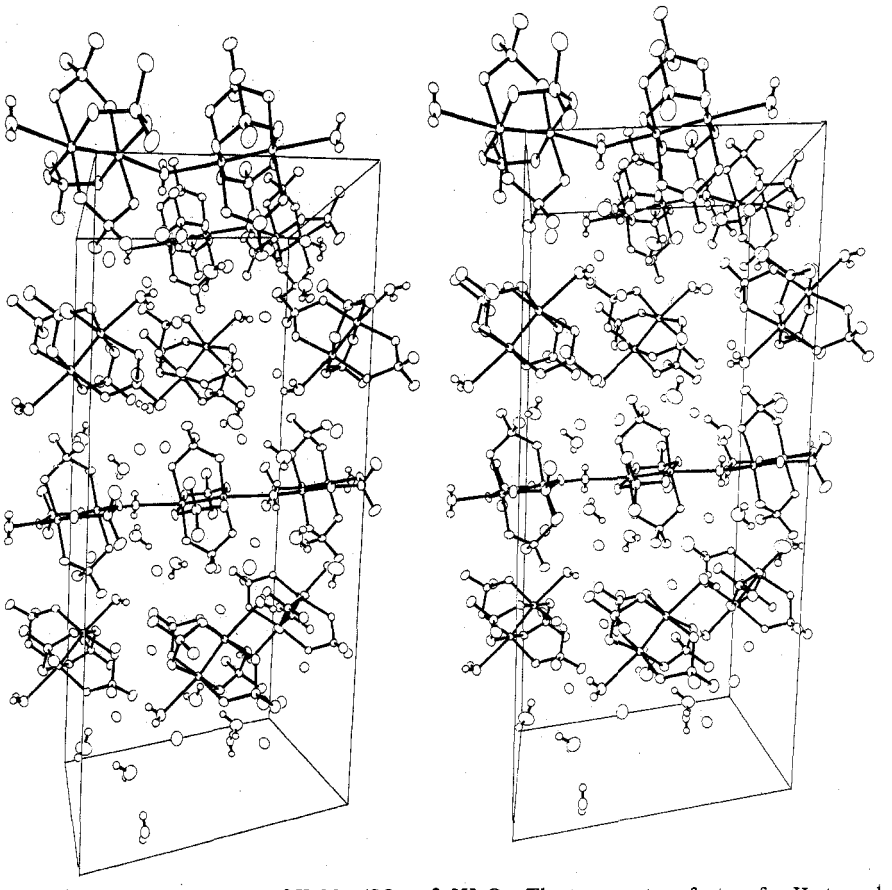

**Figure 7.** Stereoscopic view of the unit cell constants of $K_3Mo_2(SO_4)_4 \cdot 3.5H_2O$. The temperature factors for H atoms have been set at 1.0 Å$^2$. The complexes centered in the *bc* plane have been omitted.

**Table X.** Bond Angles (deg) in $K_4Mo_2(SO_4)_4 \cdot 2H_2O$

| | | | |
|---|---|---|---|
| Mo-Mo-O(1,1) | 93.6 (2) | Mo-O(2,1)-S(2) | 120.8 (2) |
| Mo-Mo-O(1,2) | 94.9 (2) | Mo-O(2,2)-S(2) | 119.9 (2) |
| Mo-Mo-O(2,1) | 94.2 (1) | O(1,1)-S(1)-O(1,2) | 106.8 (2) |
| Mo-Mo-O(2,2) | 94.2 (1) | O(1,1)-S(1)-O(1,3) | 109.1 (3) |
| Mo-Mo-O(2,4)′ | 173.9 (1) | O(1,1)-S(1)-O(1,4) | 109.3 (3) |
| O(1,1)-Mo-O(1,2) | 171.4 (1) | O(1,2)-S(1)-O(1,3) | 109.1 (3) |
| O(1,1)-Mo-O(2,1) | 91.5 (2) | O(1,2)-S(1)-O(1,4) | 109.0 (3) |
| O(1,1)-Mo-O(2,2) | 88.2 (2) | O(1,3)-S(1)-O(1,4) | 113.3 (3) |
| O(1,1)-Mo-O(2,4)′ | 81.7 (2) | O(2,1)-S(2)-O(2,2) | 107.3 (2) |
| O(1,2)-Mo-O(2,1) | 87.2 (2) | O(2,1)-S(2)-O(2,3) | 109.8 (3) |
| O(1,2)-Mo-O(2,2) | 91.9 (2) | O(2,1)-S(2)-O(2,4) | 107.9 (2) |
| O(1,2)-Mo-O(2,4′) | 89.8 (2) | O(2,2)-S(2)-O(2,3) | 109.5 (3) |
| O(2,1)-Mo-O(2,2) | 171.6 (1) | O(2,2)-S(2)-O(2,4) | 110.5 (3) |
| O(2,1)-Mo-O(2,4)′ | 89.8 (1) | O(2,3)-S(2)-O(2,4) | 111.7 (3) |
| O(2,2)-Mo-O(2,4)′ | 81.8 (1) | S(2)′-O(2,4)′-Mo | 126.4 (3) |
| Mo-O(1,1)-S(1) | 119.7 (2) | H(1)-O(3)-H(2) | 107 (7) |
| Mo-O(1,2)-S(1) | 118.8 (2) | | |

**Table XI.** Selected Interatomic Distances (Å) in $K_3Mo_2(SO_4)_4 \cdot 3.5H_2O$

| | Molecule 1 | Molecule 2 |
|---|---|---|
| Mo-Mo | 2.167 (1) | 2.162 (1) |
| Mo-O(T) | 2.550 (4) | 2.545 (3) |
| Mo-O(1,1) | 2.084 (3) | 2.055 (3) |
| Mo-O(1,2) | 2.069 (3) | 2.066 (3) |
| Mo-O(2,1) | 2.070 (3) | 2.076 (3) |
| Mo-O(2,2) | 2.046 (3) | 2.051 (4) |
| S(1)-O(1,1) | 1.518 (4) | 1.522 (4) |
| S(1)-O(1,2) | 1.522 (4) | 1.524 (4) |
| S(1)-O(1,3) | 1.440 (4) | 1.435 (4) |
| S(1)-O(1,4) | 1.448 (4) | 1.442 (4) |
| S(2)-O(2,1) | 1.519 (4) | 1.515 (4) |
| S(2)-O(2,2) | 1.523 (3) | 1.527 (4) |
| S(2)-O(2,3) | 1.451 (4) | 1.448 (4) |
| S(2)-O(2,4) | 1.436 (4) | 1.436 (4) |

ments from 60 to 300 K at different field strengths show that the substance is a simple paramagnet following the Curie law.

**Table XII.** Selected Bond Angles (deg) in $K_3Mo_2(SO_4)_4 \cdot 3.5H_2O$

| | Molecule 1 | Molecule 2 |
|---|---|---|
| Mo-Mo-O(T) | 171.7 (1) | 169.6 (1) |
| Mo-Mo-O(1,1) | 92.9 (1) | 94.4 (1) |
| Mo-Mo-O(1,2) | 94.3 (1) | 93.2 (1) |
| Mo-Mo-O(2,1) | 93.9 (1) | 93.4 (1) |
| Mo-Mo-O(2,2) | 93.2 (1) | 93.5 (1) |
| O(1,1)-Mo-O(1,2) | 172.9 (1) | 172.3 (1) |
| O(2,1)-Mo-O(2,2) | 172.5 (1) | 173.1 (1) |
| O(1,1)-Mo-O(2,1) | 87.7 (1) | 90.1 (1) |
| O(1,2)-Mo-O(2,1) | 91.5 (1) | 90.9 (1) |
| O(1,1)-Mo-O(2,2) | 89.4 (1) | 88.5 (1) |
| O(1,2)-Mo-O(2,2) | 90.5 (1) | 89.7 (1) |
| Mo-O(1,1)-S(1) | 122.0 (2) | 119.8 (2) |
| Mo-O(1,2)-S(1) | 121.3 (2) | 120.0 (2) |
| Mo-O(2,1)-S(2) | 120.7 (2) | 121.7 (2) |
| Mo-O(2,2)-S(2) | 121.9 (2) | 122.2 (2) |
| O(1,1)-S(1)-O(1,2) | 105.8 (2) | 106.0 (2) |
| O(1,1)-S(1)-O(1,3) | 109.1 (2) | 109.0 (2) |
| O(1,1)-S(1)-O(1,4) | 108.6 (2) | 107.9 (2) |
| O(1,2)-S(1)-O(1,3) | 109.8 (2) | 109.6 (2) |
| O(1,2)-S(1)-O(1,4) | 109.0 (2) | 107.9 (2) |
| O(1,3)-S(1)-O(1,4) | 114.2 (2) | 115.9 (2) |
| O(2,1)-S(2)-O(2,2) | 105.6 (2) | 104.8 (2) |
| O(2,1)-S(2)-O(2,3) | 109.1 (2) | 108.6 (2) |
| O(2,1)-S(2)-O(2,4) | 110.1 (2) | 110.8 (2) |
| O(2,2)-S(2)-O(2,3) | 110.0 (2) | 107.9 (3) |
| O(2,2)-S(2)-O(2,4) | 107.7 (2) | 109.5 (2) |
| O(2,3)-S(2)-O(2,4) | 114.0 (2) | 114.8 (3) |

The magnetic moment per formula unit is 1.65 ± 0.01 BM, which corresponds to an average *g* value of 1.90 ± 0.01 if the ground state is, as expected, a spin doublet.

The interpretation of the esr spectra closely follows the discussion[8] of the spectra of $[Tc_2Cl_8]^{3-}$. A dimeric molybdenum complex with the naturally occurring isotope composition consists of six magnetically different species as outlined in Table XIII. Some evident features of Figure 2 are the

**Table XIII.** Magnetically Different Molybdenum Dimers[a]

| Compn | % abundance | $I^1$ | $I^2$ | $\mu^1$ | $\mu^2$ |
|---|---|---|---|---|---|
| Mo–Mo | 56.0 | 0 | 0 | 0 | 0 |
| $^{95}$Mo–Mo | 23.5 | $^5/_2$ | 0 | −0.9133 | 0 |
| $^{97}$Mo–Mo | 14.2 | $^5/_2$ | 0 | −0.9325 | 0 |
| $^{95}$Mo–$^{97}$Mo | 3.0 | $^5/_2$ | $^5/_2$ | −0.9133 | −0.9325 |
| $^{95}$Mo–$^{95}$Mo | 2.5 | $^5/_2$ | $^5/_2$ | −0.9133 | −0.9133 |
| $^{97}$Mo–$^{97}$Mo | 0.9 | $^5/_2$ | $^5/_2$ | −0.9325 | −0.9325 |

[a] The symbol Mo without a superscript refers to nonmagnetic nuclei.

**Table XIV.** Spin Hamiltonian Parameters[a] for $Mo_2(SO_4)_4^{3-}$

| $g_{\parallel}$ | $g_{\perp}$ | $g_{av}$(calcd) | $10^4\lvert A_{\parallel}\rvert$, cm$^{-1}$ | $10^4\lvert A_{\perp}\rvert$, cm$^{-1}$ |
|---|---|---|---|---|
| 1.891 | 1.909 | 1.903 | 45.2 | 22.9 |

[a] The values of $\lvert A_{\parallel}\rvert$ and $\lvert A_{\perp}\rvert$ refer to $^{95}$Mo with $\mu = -0.9133$.

intense perpendicular orientation line at 3400 G from the complexes with $J = I^1 + I^2 = 0$ and the four outer parallel orientation lines at 3185, 3235, 3635, and 3685 G from complexes with $J = 5$. The negative deflection at 3268 G is the perpendicular orientation line corresponding to the line at 3185 G. The Q-band spectrum, Figure 3, shows furthermore the four outer perpendicular orientation lines at 13072, 13098, 13176, and 13202 G of species with $J = {}^5/_2$, the two low-field perpendicular lines at 13008 and 13033 G of $J = 5$, and the parallel line at 13260 G from $J = 0$. From these assignments we obtained preliminary values of the parameters in the spin Hamiltonian

$$\mathcal{H} = \mu[g_{\parallel}H_zS_z + g_{\perp}(H_xS_x + H_yS_y)] + A_{\parallel}S_zJ_z + A_{\perp}(S_xJ_x + S_yJ_y)$$

Computer simulations[8] using these parameters and including the six species in Table XIII showed that only minor adjustments of the parameters were required. We assumed in these simulations that $^{95}$Mo–$^{97}$Mo complexes had hyperfine coupling parameters halfway between those of $^{95}$Mo–$^{95}$Mo and $^{97}$Mo–$^{97}$Mo and treated the system as if the two nuclei were equivalent. Due to the very small difference in magnetic moments of $^{95}$Mo and $^{97}$Mo this is a good approximation. This difference is revealed in the spectra only as a slight broadening in the lines from the species with $J > 0$. The final simulated X-band spectrum is almost identical with that of Figure 2, assuming the spin Hamiltonian parameters in Table XIV and adding for each step of 0.5° in the polar angle single-molecule first-derivative lorentzian lines with a width of 8 G for the species with $J > 0$ and 6 G for those with $J = 0$. It is well known that line widths may depend on the nuclear moment.[25]

The esr spectra thus show that the paramagnetic species have axial symmetry and that the single unpaired electron is evenly distributed over two magnetically equivalent molybdenum nuclei.

The $g$ factors and their correlation with electronic structure[22–24] will be the subject of a later paper.[26]

**Acknowledgment.** Support by the National Science Foundation (Grant No. 33142X) is gratefully acknowledged. Funds from The Robert A. Welch Foundation were used to purchase the X-ray diffractometer and the Beckman Electroscan 30. We thank Professor J. H. Lunsford (TAMU) for his cooperation in the use of esr facilities and Mrs. Solveig Kallesoe, Chemistry Laboratory I, The H. C. Orsted Institute, University of Copenhagen, Copenhagen, Denmark, for carrying out the measurements of magnetic susceptibilities. E. P. acknowledges a leave of absence from this institution, 1973–1974.

**Registry No.** $K_3Mo_2(SO_4)_4 \cdot 3.5H_2O$, 53260-21-2; $K_4Mo_2(SO_4)_4 \cdot 2H_2O$, 53293-19-9.

**Supplementary Material Available.** Tables I and V, giving structure factor amplitudes for $K_3Mo_2(SO_4)_4 \cdot 3.5H_2O$ and $K_4Mo_2(SO_4)_4 \cdot 2H_2O$, will appear following these pages in the microfilm edition of this volume of the journal. Photocopies of the supplementary material from this paper only or microfiche (105 × 148 mm, 24× reduction, negatives) containing all of the supplementary material for the papers in this issue may be obtained from the Journals Department, American Chemical Society, 1155 16th St., N.W., Washington, D. C. 20036. Remit check or money order for $5.00 for photocopy or $2.00 for microfiche, referring to code number AIC40408J.

## References and Notes

(1) F. A. Cotton, *Chem. Soc. Rev.*, in press.
(2) A. R. Bowen and H. Taube, *J. Amer. Chem. Soc.*, **93**, 3287 (1971).
(3) F. A. Cotton, B. A. Frenz, and L. W. Shive, *Inorg. Chem.*, in press.
(4) C. L. Angell, F. A. Cotton, B. A. Frenz, and T. R. Webb, *J. Chem. Soc., Chem. Commun.*, 399 (1973).
(5) F. A. Cotton, B. A. Frenz, and T. R. Webb, *J. Amer. Chem. Soc.*, **95**, 4431 (1973).
(6) J. V. Brencic and F. A. Cotton, *Inorg. Chem.*, **9**, 351 (1970).
(7) F. A. Cotton, B. A. Frenz, and Z. C. Mester, *Acta Crystallogr., Sect. B*, **29**, 1515 (1973).
(8) Parts I and II: F. A. Cotton and E. Pedersen, *Inorg. Chem.*, **14**, 383, 388 (1975).
(9) R. S. Nicholson, *Anal. Chem.*, **37**, 1351 (1965).
(10) R. S. Nicholson and I. Shain, *Anal. Chem.*, **36**, 706 (1964).
(11) F. A. Cotton, B. A. Frenz, G. Deganello, and A. Shaver, *J. Organometal. Chem.*, **50**, 227 (1973).
(12) The following computer programs were used: DATARED by Frenz for data reduction; FAME, a program for calculating normalized structure factors by Dewar; JIMDAP, a version of Zalkin's Fourier program FORDAP, as modified by Ibers; NUCLS, a full-matrix least-squares program by Ibers and Doedens, based on Busing and Levy's ORFLS program; RSCAN by Doedens for analysis of structure factors; ORTEP by Johnson for illustrations; ORFFE by Busing, Martin, and Levy as modified by Brown, Johnson, and Thiessen for distances and angles; LIST by Snyder for listing structure factors for publication.
(13) D. T. Cromer and J. T. Waber, "International Tables for X-Ray Crystallography", Vol. IV, Kynoch Press, Birmingham, England, in press.
(14) R. F. Stewart, E. R. Davidson, and W. T. Simpson, *J. Chem. Phys.*, **42**, 3175 (1965).
(15) J. A. Ibers and W. C. Hamilton, *Acta Crystallogr.*, **17**, 781 (1964).
(16) D. T. Cromer and D. Liberman, *J. Chem. Phys.*, **53**, 1891 (1970).
(17) See paragraph at end of paper regarding supplementary material.
(18) D. Lawton and R. Mason, *J. Amer. Chem. Soc.*, **87**, 921 (1965); F. A. Cotton, Z. C. Mester, and T. R. Webb, *Acta Crystallogr.*, in press.
(19) F. A. Cotton and J. G. Norman, Jr., *J. Coord. Chem.*, **1**, 261 (1971); *J. Amer. Chem. Soc.*, **94**, 5697 (1972).
(20) L. Ricard, P. Karagiannides, and R. Weiss, *Inorg. Chem.*, **12**, 2179 (1973).
(21) C. N. Morimoto and E. C. Lingafelter, *Acta Crystallogr., Sect. B*, **26**, 335 (1970); U. Thewalt, *ibid.*, **27**, 1744 (1971).
(22) F. A. Cotton, *Inorg. Chem.*, **4**, 334 (1965).
(23) F. A. Cotton and C. B. Harris, *Inorg. Chem.*, **6**, 924 (1967).
(24) J. G. Norman, Jr., and H. J. Kolari, *J. Chem. Soc., Chem. Commun.*, 303 (1974).
(25) H. A. Kuska and M. T. Rogers in "Coordination Chemistry," Vol. 1, A. E. Martell, Ed., Van Nostrand, New York, N. Y., 1971, p 186.
(26) F. A. Cotton and E. Pedersen, *J. Amer. Chem. Soc.*, in press.